Device for Simultaneous Wind and Raindrop Energy Harvesting Operating on the Surface of Plant Leaves

Serena Armiento, *Student Member, IEEE*, Fabian Meder, *Member, IEEE*, and Barbara Mazzolai, *Member, IEEE*

***Abstract*—Soft (bio)hybrid robotics aims at interfacing living beings with artificial technology. It was recently demonstrated that plant leaves coupled with artificial leaves of selected materials and tailored mechanics can convert wind-driven leaf fluttering into electricity. Here, we significantly advance this technology by establishing the additional opportunity to convert kinetic energy from raindrops hitting the upper surface of the artificial leaf into electricity. To achieve this, we integrated an extra electrification layer and exposed electrodes on the free upper surface of the wind energy harvesting leaf that allow to produce a significant current when droplets land and spread on the device. Single water drops create voltage and current peaks of over 40V and 15μA and can directly power 11 LEDs. The same structure has the additional capability to harvest wind energy using leaf oscillations. This shows that environment-responsive biohybrid technologies can be tailored to produce electricity in challenging settings, such as on plants under motion and exposed to rain. The devices have the potential for multisource energy harvesting and as self-powered sensors for environmental monitoring, pointing at applications in wireless sensor networks (WSNs), the Internet of Things (IoT), smart agriculture, and smart forestry.**

***Index Terms*—Soft robot materials and design, biologically-inspired robots, biomimetics, soft sensors and actuators, environment monitoring and management.**

I. Introduction

EFFICIENT management and protection of the Earth's limited resources depends on sustainable technologies and effective monitoring of the environment: distributed sensor networks and robotics are among the promising tools that can face these challenges. [1], [2] During this process, sustainability is key: this translates both in biodegradable materials as well as off-grid access to clean energy supplies. The environment provides several opportunities to replace traditional power supplies such as batteries, which require periodic maintenance and dedicated disposal. [3] Energy harvesters based on triboelectric nanogenerators (TENGs), for example, collect charges resulting from vibration and movement and transform them into current. [4], [5], [6], [7] Recently, it has been reported that also plant leaves can perform a similar energy conversion as TENGs due to the leaf's materials and structure. [8] Energy harvesters can be created by enhancing the output of the leaves with soft, transparent, and organism-compatible materials in the shape of artificial leaves which are installed on the surface of the plant leaf. Actuated by wind, the two surfaces flutter and establish transient contact and separation which produces charges both on the leaf cuticle and the harvester, that can be collected. Details on the mechanism are presented in Refs. [8], [9], [10] The use of living plant leaves reduces the consumption of artificial materials as part of the triboelectric pair. [8], [11], [12], [13] However, extreme environments like high humidity or wet surfaces reduce the ability of two contacting solid materials to charge triboelectrically. Although the effect is reversible in dry environments, improvements are required to counterbalance the adverse effect of rainfall, especially when envisioning outdoor applications. A possible solution could be compensating the reduction of harvested energy by using the kinetic energy associated with raindrops as additional energy source. Raindrop energy harvesting can be achieved as follows: water droplets can triboelectrically charge a material surface (often fluorinated polymers) while spreading on it. The spreading and shrinking droplets act additionally as a surface area-changing electrode that transiently connects to electrodes exposed on the surface creating a current. [14], [15] Energy conversion efficiencies of ~ 2% have been reported and single droplets have been shown to directly power multiple LEDs during the impact.[16] Here we improve and expand our previous wind energy harvesting plant-hybrid generator by establishing extra rain energy harvesting structures on its upper surface. The additional, raindrop energy harvesting structure expectedly does not prevent the decrease of solid-solid triboelectrification on wet surfaces. However, it mitigates a potential energy reduction by harvesting

Manuscript received 28 October 2022; accepted 12 February 2023. Date of publication 28 February 2023; date of current version 9 March 2023. This letter was recommended for publication by Associate Editor Y. Chen and Editor X. Liu upon evaluation of the reviewers' comments. Research supported by the GrowBot project, the European Union's Horizon 2020 Research and Innovation Programme under Grant 824074. *(Corresponding authors: Fabian Meder; Barbara Mazzolai.)*

Serena Armiento is with the Biorobotics doctorate of Scuola Superiore Sant'Anna, 56025 Pisa, Italy, also with the Bioinspired Soft Robotics group at the Italian Institute of Technology, 16163 Genova, Italy (e-mail: serena.armiento@iit.it).

Fabian Meder and Barbara Mazzolai are with Bioinspired Soft Robotics group at the Italian Institute of Technology, 16163 Genova, Italy (e-mail: fabian.meder@iit.it; barbara.mazzolai@iit.it).

This letter has supplementary downloadable material available at https://doi.org/10.1109/LRA.2023.3250006, provided by the authors.

Digital Object Identifier 10.1109/LRA.2023.3250006

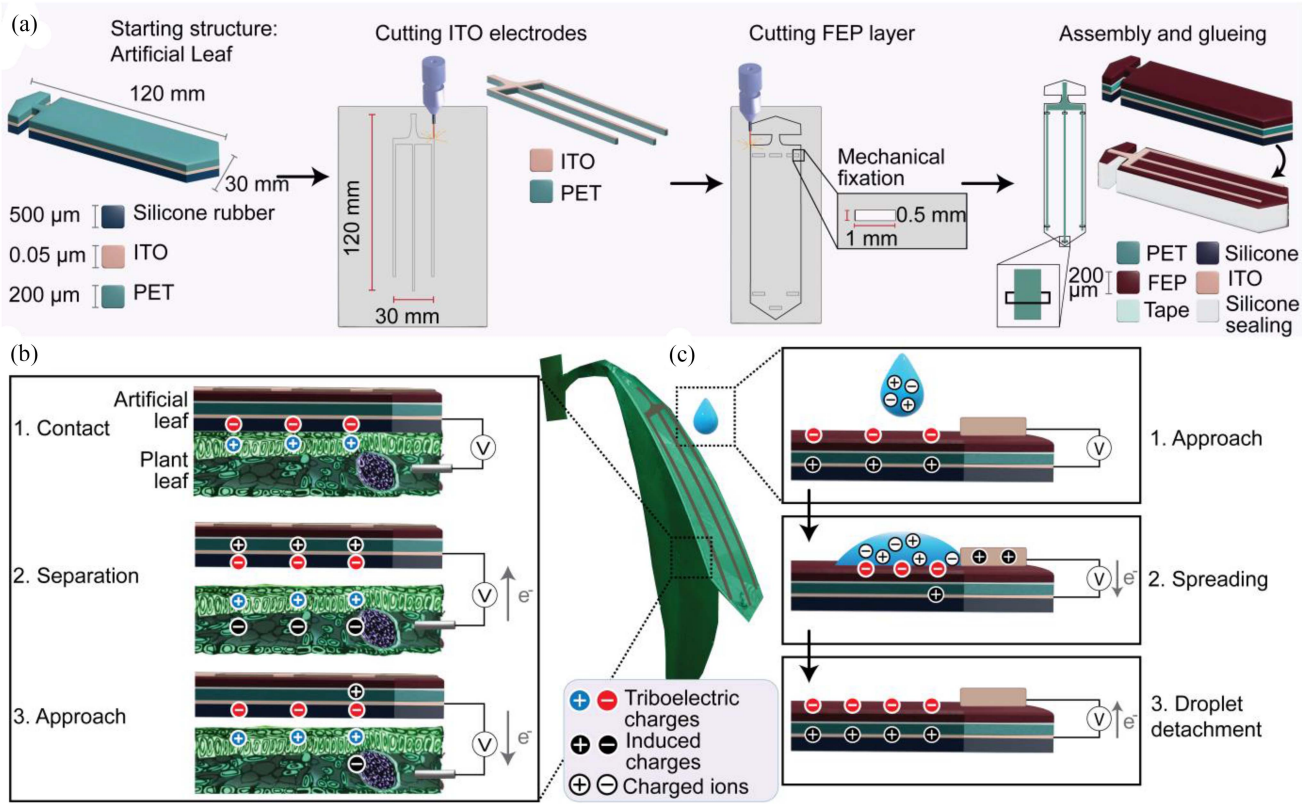

Fig. 1. Assembly and working mechanism of the plant-hybrid harvester for wind and rain energy harvesting. a) Fabrication process for implementing a rain energy conversion structure on the top of the wind energy harvesting artificial leaf by assembly of a laser-cut transparent electrode and the FEP electrification layer. Dimensions of the prototype and the single layers are included. b) Mechanism of wind energy conversion occurring on bottom of the artificial leaf and on top of the plant leaf based on solid-solid triboelectrification upon wind-driven transient contact between them. The legend shows the triboelectric charges generated on the surface and the induced charges in the plant tissue and the ITO electrode, respectively. c) Mechanism for raindrop energy conversion occurring on top of the artificial leaf based on liquid-solid contact electrification. When the droplet hits the charged FEP layer, it spreads, triboelectrically charges the FEP, connects to the surface electrode, and the charged ions in the droplet transiently compensate surface charges forming a capacitor with the sandwiched electrode.

energy directly from the droplet itself when wind and rain occur simultaneously. In fact, the highest performance was achieved under simultaneous stimulation by water droplets and air flow. We characterize the effect of structural, material and droplet parameters on the rain energy conversion and how it couples with the wind energy harvesting. The dual-source plant-hybrid energy harvester has potential as self-powered environmental sensor and as off-grid energy source. Plants become active parts of the energy conversion mechanism, enabling applications in plant ecosystems and agriculture. Such technologies enter in the framework of soft robotics, which aims at creating a new generation of (bio)hybrid robots that interact effectively with living beings and allow to implement non-native functionalities.[17], [18], [19], [20], [21], [22], [23], [24]

II. Assembly of the Energy Harvester

A. Artificial Leaf for Wind and Rain Energy Harvesting

The artificial leaf was realized using soft and transparent multilayered materials, here a 0.5 mm silicone elastomer layer on top of a ∼100 nm indium-tin oxide (ITO) electrode deposited on a 0.2 mm polyethylene-terephthalate (PET) sheet. Details are described elsewhere [9], [10] On top, a structure to enable rain energy harvesting was established as illustrated in Fig. 1(a): a thin layer of ITO-coated PET (thickness 200 µm, nominal sheet resistance 350-500 Ωsquare-1, ThorLabs Inc., USA) was cut into the desired shape using a laser cutter (Flux BEAMO, Belgium). Similarly, a 150 µm sheet of fluorinated ethylene propylene (FEP, UniTak3D, Shenzhen, China) was cut in the shape of the artificial leaf. Moreover, rectangular windows were cut on the upper and lower part of the FEP layer to allow mechanical fixation of the ITO electrode (as highlighted in steps 2 & 3 of Fig. 1(a)). The ITO-FEP layer is adhered onto the PET surface of the previous prototype using double-sided tape or adequate liquid glue. Finally, a thin layer of silicone rubber adhesive (SilPoxy, Smooth-On, Pennsylvania, USA) was distributed over the edges of the device to seal the device and prevent electric contact of the inner electrodes with water droplets.

B. Application of the Artificial Leaf on Plants

The artificial leaves have been firmly fixed at the petiole of a leaf of a *Nerium oleander* plant using silicone tape in a manner that both lamina (of the artificial and plant leaf) can freely move and interact upon fluttering in wind. [9], [10]

III. Mechanisms for Energy Harvesting

A. Wind Energy Harvesting

Fig. 1(b) illustrates the mechanism of wind energy harvesting: upon contact of the artificial leaf with the plant leaf, the surfaces of the silicone elastomer and the leaf cuticle charge net negatively and net positively, respectively as analyzed in detail previously.[8] When the leaf and the energy harvester are subsequently separated, the surface charges are electrostatically induced into the adjacent electrode forming opposite charges. This causes a current flow between the electrodes. When the fluttering brings the two surfaces back in contact, the charges on the respective surfaces re-establish an electrostatic equilibrium resulting in an opposite current flow between the electrodes.

B. Rain Energy Harvesting

The conversion of the kinetic energy of single water drops into electricity occurs on the top surface of the artificial leaf, as illustrated in the schematic of Fig. 1(c). Here we implemented a structure composed of a triboelectrically active FEP layer and an electrode. FEP charges negatively upon contact with a water droplet through liquid-solid contact electrification.[14], [15] These charges are electrostatically induced into the sandwiched electrode also used for wind energy harvesting and into the droplet where oppositely charged ions in the droplet rearrange compensating the surface charges. However due to the top electrodes an additional mechanism occurs. The droplet's kinetic energy causes it to spread on the FEP layer and subsequently to shrink back. During these motions, the droplet contacts the top electrode forming a droplet spreading area-dependent half-electrode of a capacitor together with the inner ITO electrode and the charged FEP layer. Droplet dynamics change the electrode area of the capacitor, thus varying its capacitance. The new electrostatic equilibrium formed at the surface due to the charge-screening of the droplet causes a flow of charges between the two electrodes. The charge accumulated by the capacitor thus likely depends on the surface covered by the droplet, the surface charge, the ion concentration, and the kinetic energy at the moment of impact. As the droplet detaches from the electrode and leaf surfaces, the capacitive coupling changes, the surface charges on the FEP layer lead to the formation of charges in the sandwiched electrode, and a current of opposite polarity is observed. The FEP's hydrophobic properties support efficient removal of the water droplets. The mechanism reoccurs when the next droplet lands on the artificial leaf.

IV. Data Acquisition and Analysis

The performance and critical parameters regarding the composition and structure of the artificial leaf were tested using a custom experimental setup.

A. Experimental Setup

All tests were carried out in a Faraday cage, consisting of an aluminum frame covered with a fine meshed copper mesh for electromagnetic shielding (Thorlabs Inc., New Jersey, USA). Water droplets were generated using a syringe pump (BI-SEP-P1000, Linari NanoTech, Italy) using a 60 mL syringe connected to a silicone tube at which end was an electrically grounded metal outlet installed. The outlet was connected to the ground to remove possible charges formed by the friction of the liquid against the silicone tube. [25], [26] The resulting uncharged droplets were falling from a height of typically 80 cm (or varying height as indicated) onto the artificial leaf.

Most experiments were carried out with a droplet dispensing frequency of 45 ml/min (∼200 droplets per minute) if not otherwise indicated. In addition, we tested energy storage in a capacitor at droplet frequencies between 20 and 420 droplets/min. The value of 200 droplets/min was chosen to reduce experimentation time by increasing the droplet signals measured per time interval while still recording each single droplet signal in high resolution. Moreover, it provided the best electrification of the device surface and an acceptable removal of droplets from the device. The top and bottom electrode of the artificial leaf were connected to an electrometer (6517B, Keithley, USA) and to an oscilloscope (MSO7014A, Agilent Technologies, USA) to analyze voltage, current, and transferred charges. All data was analyzed using MATLAB R2022a. Snapshots illustrating the interaction between water droplets and the device were obtained by high-speed camera videos recorded using a Phantom Miro C110 (Phantom Ametek, New Jersey, USA) at a frame rate of 1200 frames per second (fps). A few drops of water-soluble black ink were added to the water reservoir to increase the contrast during video recordings.

V. Results and Discussion

A. Effect of Artificial Leaf Structure on Raindrop Energy Harvesting

Here, our analysis focusses on the investigation of the raindrop energy harvesting capability, as the wind energy harvesting capability of the artificial leaf has been analyzed in detail before [8], [9], [10]. It is essential to investigate the surface triboelectric material and the dimensions of the top electrode as they are considered crucial for its performance and the results are shown in Fig. 2. First, we studied the effect of the number of segments of the top electrode (Fig. 2(a)) as this could influence the probability that a droplet contacts the electrode during spreading on the surface. Thus, the ideal number of segments depends also on the droplet spreading area and the dimensions of the artificial leaf and can be easily adapted to its shape and size. Our artificial leaf was dimensioned to be applied on *N. oleander* leaves, resembling the shapes and size of their natural host (surface area of artificial leaf: 3225 mm²). Top electrodes with one, three, and five segments were tested in terms of current and voltage generated when droplets hit the artificial leaf in a central position at a rate of ∼200 droplets per minute (Fig. 2(a)). Single- and triple-segmented electrodes obtained comparable results (mean voltage and mean current: 15 V and 2.5 μA), while the electrode with five segments resulted in both, decreased currents and voltages, respectively (mean voltage and mean current: 5 V and 1 μA). This could indicate that too many top electrodes hinder spreading of the droplet reducing the active surface area for energy conversion. Furthermore, the

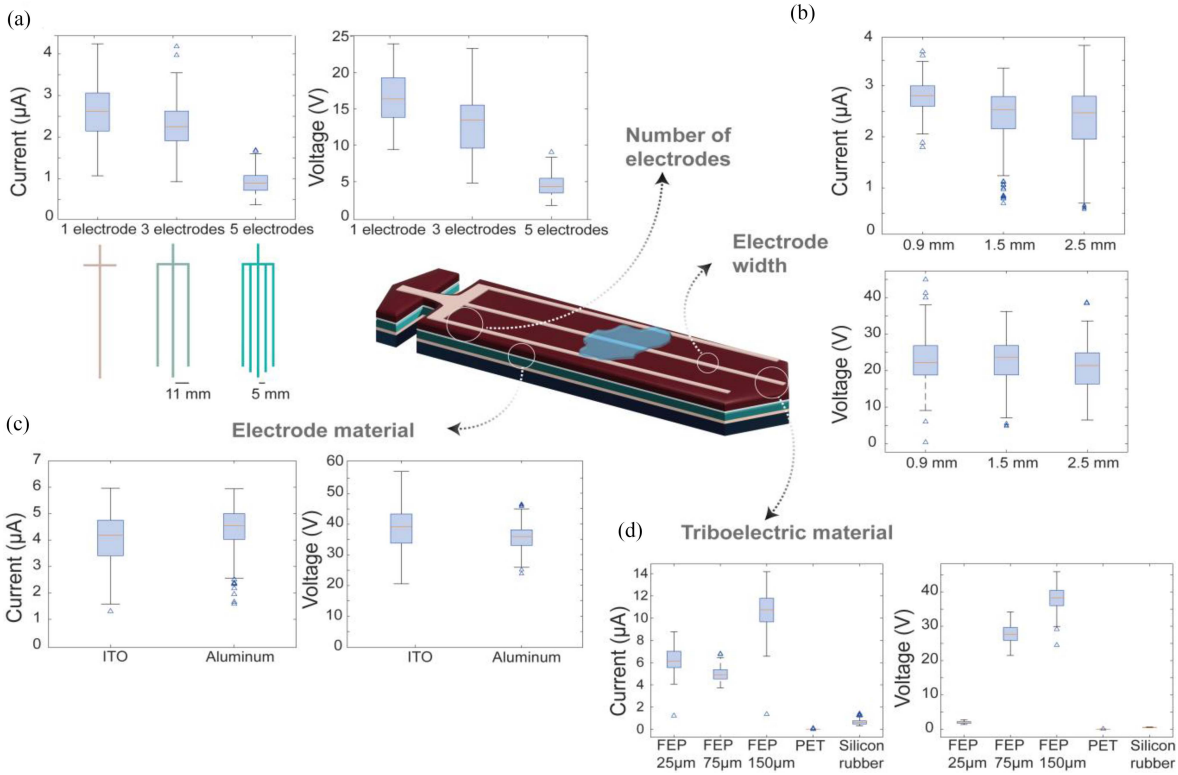

Fig. 2. Effect of upper artificial leaf structure on water drop energy conversion and device performance. a) Influence of the number of electrode segments on current and voltage generated upon DI water droplet impact. The graphics illustrate the electrode shapes and distance between the segments. b) Influence of electrode width on current and voltage generated on a structure with a single electrode upon DI water droplet impact. c) Effect of the electrode material (metallic or metal oxide conductor) on current and voltage generated upon DI water droplet impact. d) Effect of triboelectrification materials under the top electrode on the current and voltage generated. All boxplots summarize the statistics of measurements from ~∼160 droplets, the bars indicate the maximum and minimum values while the triangles represent the outliers.

results indicate that in our experiments ∼10 mm between the single segments of the electrode is optimal for a device width of 30 mm. Vertical segments were preferred over horizontal ones as the vertical structures improved the sliding motion of the droplets along the device and thus improved the droplet removal from the surface. Moreover, the given shape facilitated fabrication. However, that does not exclude that other electrode configurations which assure contact with the spreading droplet and allow for the droplet to slide off from the surface could be used as well or even exploited to further tune the output, by adapting electrode shape and distance for example to other droplet spreading areas. Fig. 2(b) shows that the electrode width (when varied between 0.9 and 2.5 mm using a single electrode segment) changes the electrical output only marginally. Hence, a width of 0.9 mm was chosen for the subsequent prototypes. Moreover, we did not find any significant difference when performing experiments with metal electrodes instead of ITO as top electrodes (Fig. 2(c)). We thus used ITO-coated PET due to its transparency, flexibility, and ease of fabrication of complex shapes by laser cutting. In addition, considering the varying dry-wet and hence harsh conditions to which the artificial leaf can be exposed to, some metal electrodes may corrode or form a resistive layer on the surface which could hinder the efficacy in the long term. We tested the conductivity of the ITO layer after exposure to DI water for 21 days and conductivity changed insignificantly from 0.28 $k\Omega cm^{-1}$ to 0.27 $k\Omega cm^{-1}$ within this timeframe. This indicates that the electrode is very stable upon contact with DI water. Yet, in future, especially for outdoor applications, this investigation should be extended to a series of natural rainwater which contains higher ion concentrations and varying pH. Also the material that electrifices upon water contact crucially affects the output (Fig. 2(d)). FEP outperforms other negatively charging materials such as PTFE, silicone rubber, and PET. Moreover, FEP layers of a thickness of 150 μm performed better than thinner layers reaching current peaks of 14 μA and voltage peaks of 45 V with single droplets. This could be because the FEP acts as the dielectric in the capacitor formed together with the top electrode and bottom (sandwiched) electrode. The voltage across this capacitor scales linearly with the thickness of the dielectric increasing the output. Furthermore, electrical breakdowns in thinner dielectric layers may occur that are avoided in the thicker FEP layer. Further in-depth studies may clarify this aspect and help to further tune the power output performance of the upper triboelectric layer.

B. Effect of Droplet Composition and Impact on Energy Harvesting

Fig. 3 summarizes how the droplet composition and the impact influence water droplet energy conversion. Fig. 3(a) shows

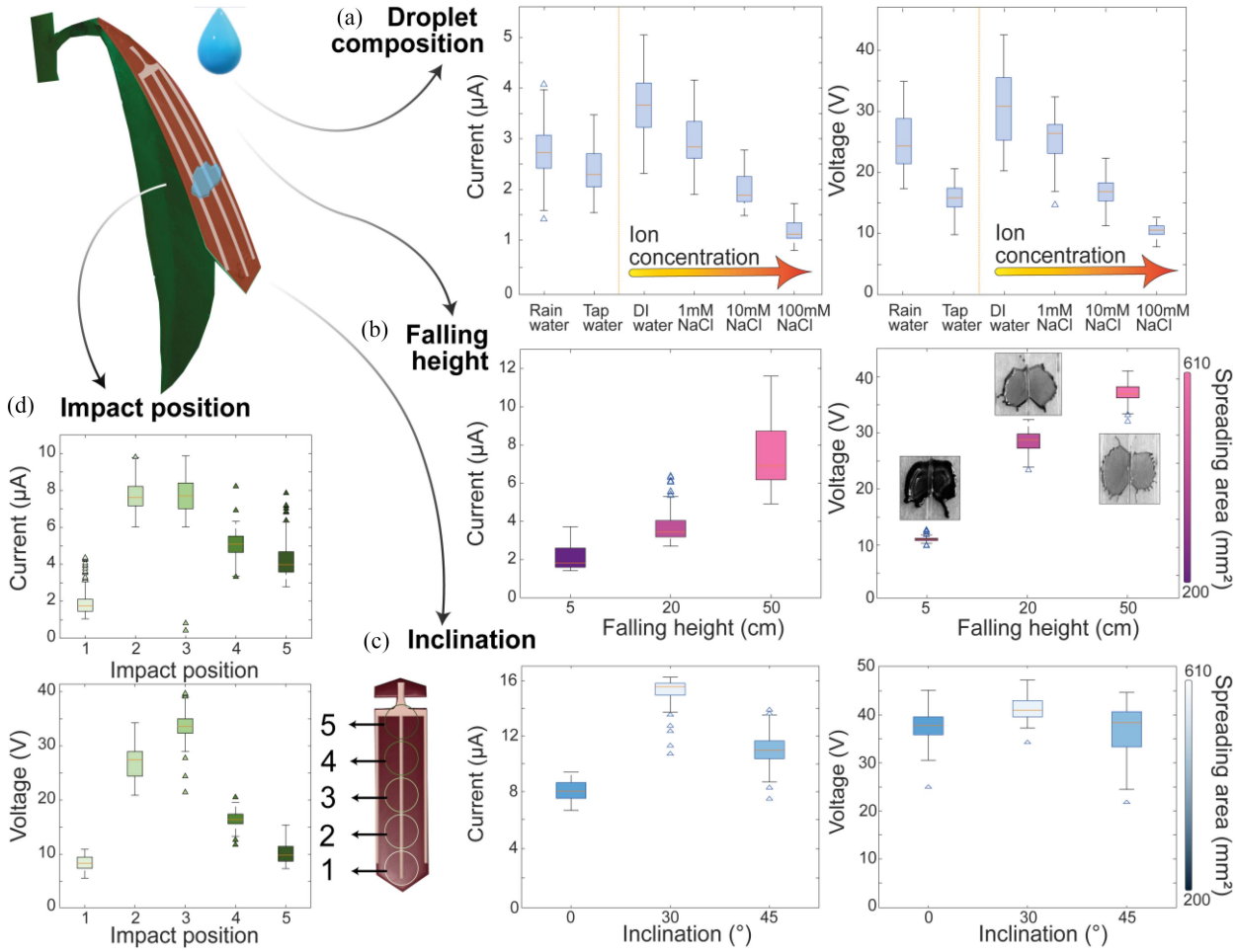

Fig. 3. Water drop energy harvesting as function of droplet composition and impact zone. a) Influence of the droplet composition and ion content on current and voltage generation. b) Effect of droplet falling height on the generated current and voltage signals. The color scale bar on the right indicates the droplet spreading area (at its maximum, average of 10 measurements). c) Influence of the device inclination angle on the current and voltage generated (0° refers to a horizontal position, 30°, and 45° indicate the angle of downwards inclination). The color scale bar on the side indicates the maximum spreading area of the droplets (average of 10 measurements). d) Effect of the droplet impact position on the corresponding current and voltage signals. The numbers and color code refer to the graphic on the right showing the five impacting positions tested. All boxplots summarize the statistics of measurements of ∼160 droplets, the bars indicate the maximum and minimum values, while the triangles represent the outliers.

tests in which rainwater, tap water, and DI water supplemented with different sodium chloride concentrations affect voltage and current signals.

As expected, higher ion concentrations reduce the transferrable charges and hence harvestable voltage and currents. Indeed, rainwater and DI water, due to the low ion concentration, are expectedly producing the highest outputs. Interestingly, a solution of 1 mM NaCl shares similar current and voltage values with the rainwater suggesting that rainwater which is not ultrapure as DI water but may contain other ions, particles etc., may have a similar electrification behavior than the 1 mM NaCl solution. As previously mentioned, the charges produced by the water drop impact depend on multiple factors, e.g., their kinetic energy ($E_k = 0.5^*m^*v^2$ where m is the mass of the droplet and v is the velocity) at the moment of impact, which in turn is mostly determined by the height (ignoring friction, $v^2 = h/2^*g$, where h is the height and g is the gravitational acceleration) from which the droplets fall. Fig. 3(b) shows the electrical measurements as well as the droplet maximal spreading area obtained from high-speed video recordings (1200 fps).

The results demonstrate that droplets falling from 5 cm have expectedly a reduced spreading area due to their lower kinetic energy and this results in reduced voltages and currents compared to droplets falling from higher distances. Indeed, the output scales almost linearly with the falling height. In natural contexts, raindrops travel even for tenths of meters before impacting with an object near the ground and thus possess much higher kinetic energies that are very difficult to replicate in a laboratory. Nonetheless, the velocity of natural raindrops is limited by the friction with air to a value called "terminal velocity" which depends on the size of the droplet and its density. [27] For droplets of 6 mm in diameter, the terminal velocity is around 12 m/s, depending on the atmosphere. The same droplets in our laboratory setup could reach ∼4 m/s. Another parameter influencing the droplet-artificial leaf interaction is the impact position and the inclination of the artificial leaf. The artificial leaf

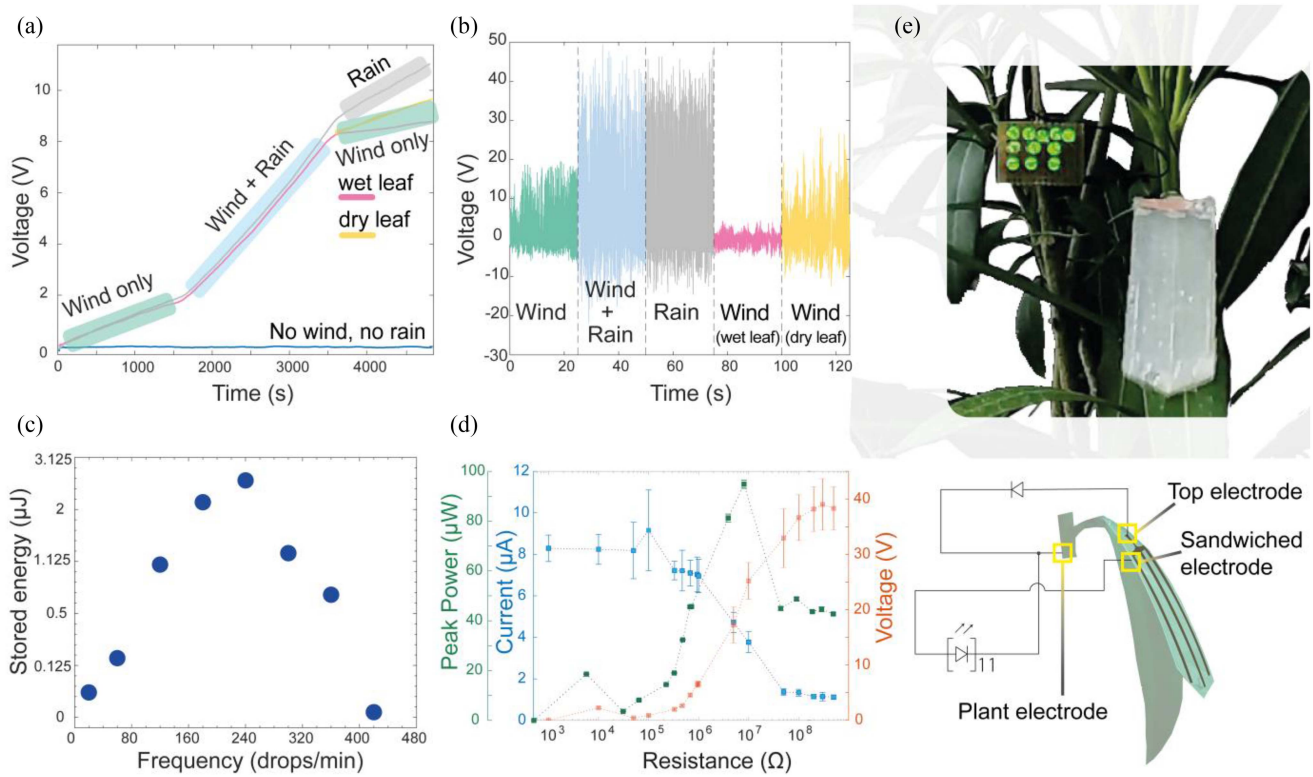

Fig. 4. Simultaneous wind and rain energy conversion. a) Charging curve of a 1μF capacitor fed by the device under "varying weather conditions" and b) the related voltages generated. Wind and rain were simulated by concurrently or separately exposing the leaves to air flow (9.8 m/s) and DI water droplets (200 drops/min), respectively. The conditions have been applied sequentially as follows, from left to right: first wind (green curve), followed by wind and rain (blue curve), followed by rain (grey curve), or followed by wind on wet leaves (pink curve) or on dry leaves (yellow curve), respectively. The blue curve in a) is the reference without wind and rain showing no charging. c) Influence of droplet frequency hitting the device on the energy stored in a capacitor within 100 seconds. d) Impedance matching: current and voltage signals and the related power peak as function of the load resistance. Mean and standard deviation of ~ 160 droplets are shown. e) A frame of Movie 1 showing the device and 11 LEDs powered by the impact of a single water drop. The schematic shows the circuit employed during the simultaneous wind and rain energy harvesting.

can adopt different inclinations depending on how it is installed on the natural leaf and as function of external forces, e.g., wind and branch movement. Fig. 3(c) shows voltage and current output of the artificial leaf at an inclination of 0° (horizontal), 30°, and 45° in downwards orientation when water is dropping on a central position. An inclination of 30° was found to result in the highest average output. Firstly, high speed videos data indicate that the different spreading areas of the droplets in the tested conditions do not vary significantly enough to explain these results. On the other hand, the droplet motion is likely influenced by the harvester's inclination and the release of the water droplets from the surface. Moreover, the elastic deformation of the flexible artificial leaf will have further complex influence on the droplet impact and release dynamics. These, in turn seem also to influence the electrical output when dropping on different positions along the central axis of the artificial leaf at 0° inclination (Fig. 3(d)). Both, current and voltage signals, are highest for droplets hitting the leaf in a central position and they decrease when going to the basal and the apical extremes (where the leaf is fixed and at its tip, respectively). Optimal current and voltage generation is found when dropping on the center of the artificial leaf and this is likely a result of a combination of maximal droplet spreading and droplet release. Especially the droplet spreading may be reduced at the extremes of the artificial leaf and the droplet may not cover the entire electrode anymore reducing the voltage and currents generated. Also, droplets sliding on the device could electrify the surface and create additional signals, but those signals would likely be smaller than those generated by droplet spreading after impact. This indicates that the droplets motion on the surface could be a tool to further tune the output if the complex influence of its dynamics on the electrical output are better understood. Nevertheless, the results clearly show the reproducible and robust performance of the devices, which reaches saturation in ~ 60 seconds and produces repeatable voltages and currents over 20000 droplets of up to 47 V and 17 μA (median of 42 V and 15.5 μA, respectively) from single water droplets.

C. *Multisource Wind and Rain Energy Harvesting*

The artificial leaf is capable of harvesting energy from wind and water drops using the lower and upper leaf surface, respectively. Both, simultaneous and separate harvesting is possible. Fig. 4(a) shows the charging kinetics of a 1 μF capacitor connected to the artificial leaf installed on a *N. oleander* plant under varying weather conditions simulated by simultaneously or separately switching droplet dispenser (rain) and air flow (wind) in our test chamber on and off. The tests were conducted

as follows: the device was initially exposed to wind only (average speed of 9.8 m/s) for 1600s. Then the droplet dispenser was switched on simultaneously with the wind (for 2000s). Subsequently, we investigated three different conditions: I) wind was turned off and rain continued (grey curve). II) the droplet dispenser was turned off and wind continued, and the leaves were wiped dry with a tissue (yellow curve). III) the droplet dispenser was turned off and wind continued but leaves remained wet from the previous droplet impacts (pink curve). This allows to estimate how the charging kinetics would be affected by varying "weather" conditions. The results show that wind and rain energy can, in fact, be collected both separately and simultaneously using the same multilayered structure whereas the simultaneous harvesting resulted in maximum charging rates (3.4 mV/s). Moreover, the droplet energy harvesting structure requires to be wetted. Thus, it cannot avoid a reduction in efficiency of the solid-solid electrification by water as indicated by the different slope of the dry leaf (charging rate of 1.1 mV/s), and the wet leaf (charging rate of 0.4 mV/s). However, the results show that drying recovers higher charging rates equivalent to those in the beginning of the experiment where the leaf has been dry. Moreover, the additional rain energy harvesting structure clearly improves the overall energy harvesting indicated by the highest charging rates when wind and rain occur simultaneously. The same behavior is also reflected in the voltage signals recorded during the same conditions shown in Fig. 4(b). Voltages from water drops and combined wind and droplets are highest at the conditions of the experiments. Certainly, the frequency of the water droplets hitting the surface plays a further role and its effect on the energy stored in the capacitor is shown in Fig. 4(c). A higher number of droplets falling on the artificial leaf per unit of time expectedly increases the charging rate initially. However, after a threshold of in our case 240 drops/min, the charging rate begins to decrease. A possible explanation is that the volume of water hitting the surface may then be too high leading to the formation of a continuous water film on the surface and causing charge screening. Yet, such high droplet rates impacting of an area of $\sim$3225 mm² (artificial leaf surface) are unlikely to occur in a natural/outdoor scenario.

D. Energy Harvesting Potential and Sensing Applications

As shown above, the artificial leaf allows thus to effectively harvest wind and rain energy simultaneously. The power output reaches a peak of 100 μW at a load resistance of 10 MΩ as derived from Fig. 4(d) giving current and voltage as function of the impedance (corresponding to 16 μW/cm² when normalized by the droplet spreading area). For wind energy harvesting, a similar maximal power output of 15 μW/cm² at 1N impact force and a load resistance of 200 MΩ has been determined using similar artificial leaf materials. [8] It is clear that these values may be improved in future by better understanding the complex dynamics of the artificial leaf motion in the wind (see [28] affected by the plant and artificial leaf's mechanical properties, weight, elastic modulus, relative length etc. in addition to the previously mentioned droplet dynamics. Supporting Movie 1 shows eleven LEDs forming the letters "IIT" being lit up by wind (average speed: 9.8 m/s), and simultaneous and separate water droplet exposure. A snapshot of LEDs illuminated by a single raindrop and the relative circuit diagram used for directly powering the LEDs is given in Fig. 4(e). The results show that energy conversion from single droplets can be clearly observed, and this suggests a certain sensing functionality, for example to detect frequency of droplets hitting the leaf and thus rain rates. Moreover, it has been previously shown that wind energy harvesting is wind speed dependent and could be used to analyze wind. Thus, the devices may have potential as environmental sensors for wind and rain, and this will be validated in dedicated outdoor experiments in the future. The peak power value achieved by a single droplet is higher than the value reported before for wind energy harvesting with the artificial leaves [8] so that not only an additional power source could be established but also the maximal power output enhanced.

VI. Conclusion

Here we present the first artificial leaf that enables energy harvesting through solid-solid contact electrification on its lower surface and liquid-solid contact electrification on its top surface. Installed and combined with living plants, the plant becomes part of the wind energy harvester, and this plant-hybrid harvester robustly enables simultaneous conversion of wind-induced leaf fluttering and of the kinetic energy of falling droplets hitting the artificial leaves into electricity. This crucially expands the capabilities of previously reported prototypes and, moreover, compensates for effects like voltage reduction due to wet surfaces during solid-solid contact electrification during rain. Furthermore, the novel artificial leaf demonstrates the potential for environmental sensing, given the dependency of the power output from the wind speed and droplet rate. The ability of the artificial leaf to light LEDs upon modest fluttering and by impact of a single raindrop, also demonstrates the opportunity for a direct visible readout. In future, outdoor tests could help to assess the suitability of the artificial leaf for applications in IoT, WSNs, as well as smart forestry and smart agriculture.

References

[1] C. Torresan et al., "A new generation of sensors and monitoring tools to support climate-smart forestry practices," *Can. J. Forest Res.*, vol. 51, no. 12, pp. 1751–1765, Dec. 2021, doi: 10.1139/cjfr-2020-0295.

[2] S. Wolfert, L. Ge, C. Verdouw, and M.-J. Bogaardt, "Big data in smart farming – A review," *Agricultural Syst.*, vol. 153, pp. 69–80, 2017, doi: 10.1016/j.agsy.2017.01.023.

[3] L. B. Kong, T. Li, H. H. Hng, F. Boey, T. Zhang, and S. Li, *Waste Energy Harvesting*. Verlag Berlin, Heidelberg, Germany: Springer, 2014, doi: 10.1007/978-3-642-54634-1 .

[4] R. D. I. G. Dharmasena et al., "Triboelectric nanogenerators: Providing a fundamental framework," *Energy Environ. Sci.*, vol. 10, no. 8, 2017, doi: 10.1039/C7EE01139C.

[5] Z. L. Wang, "From contact electrification to triboelectric nanogenerators," *Rep. Prog. Phys.*, vol. 84, no. 9, Sep. 2021, Art. no. 096502. doi: 10.1088/1361-6633/ac0a50.

[6] B. Chen, Y. Yang, and Z. L. Wang, "Scavenging wind energy by triboelectric nanogenerators," *Adv. Energy Mater.*, vol. 8, no. 10, Apr. 2018, Art. no. 1702649, doi: 10.1002/aenm.201702649.

[7] Z. L. Wang, T. Jiang, and L. Xu, "Toward the blue energy dream by triboelectric nanogenerator networks," *Nano Energy*, vol. 39, pp. 9–23, 2017. doi: 10.1016/j.nanoen.2017.06.035.

[8] F. Meder et al., "Energy conversion at the cuticle of living plants," *Adv. Funct. Mater.*, vol. 28, no. 51, Dec. 2018, Art. no. 1806689, doi: 10.1002/adfm.201806689.

[9] F. Meder, M. Thielen, A. Mondini, T. Speck, and B. Mazzolai, "Living plant-hybrid generators for multidirectional wind energy conversion," *Energy Technol.*, vol. 8, no. 7, Jul. 2020, Art. no. 2000236, doi: 10.1002/ente.202000236.

[10] F. Meder, S. Armiento, G. A. Naselli, M. Thielen, T. Speck, and B. Mazzolai, "Biohybrid generators based on living plants and artificial leaves: Influence of leaf motion and real wind outdoor energy harvesting," *Bioinspiration Biomimetics*, vol. 16, no. 5, Sep. 2021, doi: 10.1088/1748-3190/ac1711.

[11] J. G. Sun, T. N. Yang, I. S. Kuo, J. M. Wu, C. Y. Wang, and L. J. Chen, "A leaf-molded transparent triboelectric nanogenerator for smart multifunctional applications," *Nano Energy*, vol. 32, pp. 180–186, Feb. 2017, doi: 10.1016/j.nanoen.2016.12.032.

[12] D. Choi, D. W. Kim, D. Yoo, K. J. Cha, M. La, and D. S. Kim, "Spontaneous occurrence of liquid-solid contact electrification in nature: Toward a robust triboelectric nanogenerator inspired by the natural lotus leaf," *Nano Energy*, vol. 36, pp. 250–259, 2017, doi: 10.1016/j.nanoen.2017.04.026.

[13] F. Meder, A. Mondini, F. Visentin, G. Zini, M. Crepaldi, and B. Mazzolai, "Multisource energy conversion in plants with soft epicuticular coatings," *Energy Environ. Sci.*, vol. 15, no. 6, pp. 2545–2556, 2022, doi: 10.1039/D2EE00405D.

[14] D. Yoo, S. J. Kim, Y. Joung, S. Jang, D. Choi, and D. S. Kim, "Lotus leaf-inspired droplet-based electricity generator with low-adhesive superhydrophobicity for a wide operational droplet volume range and boosted electricity output," *Nano Energy*, vol. 99, 2022, Art. no. 107361, doi: 10.1016/j.nanoen.2022.107361.

[15] H. Wu, N. Mendel, D. van den Ende, G. Zhou, and F. Mugele, "Energy harvesting from drops impacting onto charged surfaces," *Phys. Rev. Lett.*, vol. 125, no. 7, Aug. 2020, Art. no. 078301, doi: 10.1103/PhysRevLett.125.078301.

[16] W. Xu et al., "A droplet-based electricity generator with high instantaneous power density," *Nature*, vol. 578, no. 7795, pp. 392–396, Feb. 2020, doi: 10.1038/s41586-020-1985-6.

[17] B. Mazzolai and C. Laschi, "A vision for future bioinspired and biohybrid robots," *Sci. Robot.*, vol. 5, no. 38, Jan. 2020, Art. no. eaba6893, doi: 10.1126/scirobotics.aba6893.

[18] C. Laschi, B. Mazzolai, and M. Cianchetti, "Soft robotics: Technologies and systems pushing the boundaries of robot abilities," *Sci. Robot.*, vol. 1, no. 1, Dec. 6, 2016, doi: 10.1126/scirobotics.aah3690.

[19] J. P. Giraldo et al., "Plant nanobionics approach to augment photosynthesis and biochemical sensing," *Nature Mater.*, vol. 13, no. 4, pp. 400–408, 2014, doi: 10.1038/nmat3890.

[20] T. T. S. Lew, V. B. Koman, P. Gordiichuk, M. Park, and M. S. Strano, "The emergence of plant nanobionics and living plants as technology," *Adv. Mater. Technol.*, vol. 5, no. 3, Mar. 2020, Art. no. 1900657, doi: 10.1002/admt.201900657.

[21] J. P. Giraldo, H. Wu, G. M. Newkirk, and S. Kruss, "Nanobiotechnology approaches for engineering smart plant sensors," *Nature Nanotechnol.*, vol. 14, no. 6, pp. 541–553, Jun. 2019. doi: 10.1038/s41565-019-0470-6.

[22] G. Dufil, I. Bernacka-Wojcik, A. Armada-Moreira, and E. Stavrinidou, "Plant bioelectronics and biohybrids: The growing contribution of organic electronic and carbon-based materials," *Chem. Rev.*, vol. 122, no. 4, Dec. 2021, pp. 4847–4883, doi: 10.1021/acs.chemrev.1c00525.

[23] E. Stavrinidou et al., "Electronic plants," *Sci. Adv.*, vol. 1, no. 10, Nov. 2015, Art. no. e1501136, doi: 10.1126/sciadv.1501136.

[24] S. D. Cezan, H. T. Baytekin, and B. Baytekin, "Self-regulating plant robots: Bioinspired heliotropism and nyctinasty," *Soft Robot.*, vol. 7, no. 4, pp. 444–450, Aug. 2020, doi: 10.1089/soro.2019.0036.

[25] S. Lin, X. Chen, and Z. L. Wang, "Contact electrification at the liquid-solid interface," *Chem. Rev.*, vol. 122, no. 5, pp. 5209–5232, Mar. 2022, doi: 10.1021/acs.chemrev.1c00176.

[26] M. D. Sosa et al., "Liquid-polymer triboelectricity: Chemical mechanisms in the contact electrification process," *Soft Matter*, vol. 16, no. 30, pp. 7040–7051, Aug. 2020, doi: 10.1039/d0sm00738b.

[27] M. A. Serio, F. G. Carollo, and V. Ferro, "Raindrop size distribution and terminal velocity for rainfall erosivity studies. A review," *J. Hydrol.*, vol. 576, pp. 210–228, 2019. doi: 10.1016/j.jhydrol.2019.06.040.

[28] F. Meder, G. A. Naselli, and B. Mazzolai, "Wind dynamics and leaf motion: Approaching the design of high-tech devices for energy harvesting for operation on plant leaves," *Front. Plant Sci.*, vol. 13, 2022, Art. no. 4212, doi: 10.3389/fpls.2022.994429.